Influence of steam jet-cooking on the rheological properties of dry and wet cationized starch solutions

Carbohydrate Polymers 285 (2022) 119262

Contents lists available at ScienceDirect

Carbohydrate Polymers

journal homepage: www.elsevier.com/locate/carbpol

Influence of steam jet-cooking on the rheological properties of dry and wet cationized starch solutions☆

Martin Gabriel [a], Florian Gomernik [a], Esther Ferstl [b], Angela Chemelli [b], Roland Kádár [c,*], Stefan Spirk [a,*]

[a] Institute of Bioproducts and Paper Technology, Graz University of Technology, Inffeldgasse 23, 8010 Graz, Austria
[b] Institute of Inorganic Chemistry, Graz University of Technology, Stremayrgasse 9, 8010 Graz, Austria
[c] Department of Industrial and Materials Science, Chalmers University of Technology, 412 96 Gothenburg, Sweden

ARTICLE INFO

Keywords:
Jet-cooking
Cationic starch
Dissolution
Rheology
Dry cationization
Wet cationization
Anti-thixotropy (rheopexy)

ABSTRACT

Steam jet-cooking allows for efficient dissolution of cationic starch in paper production as it operates above the boiling point of water at elevated pressures. However, the processes involved during jet-cooking and its consequences on dissolution and finally paper properties have not been fully resolved so far. As cationic starch is the most important paper additive in the wet end, any energy or material savings during dissolution will enhance the ecologic and economic performance of a paper mill. Here, we address the topic of solubilization of four different industrially relevant cationic starches processed via steam jet-cooking. We showcase that rheology is a useful tool to assess the solubility state of starches. Some starches featured liquid-like rheological behavior (loss moduli, G'', greater than storage moduli, G') in linear viscoelastic tests and anti-thixotropic behavior in hysteresis loop tests. In contrast, cationic corn starches exhibited gel-like behavior ($G' > G''$) and negligible hysteresis directly after cooking.

Hypotheses: To evaluate the decisive factors for complete dissolution of industrial cationic starches using jet-cooking and to correlate them to rheological properties.

1. Introduction

Cationic starch (CS) ethers are one of the most important additives in the wet-end of paper manufacturing. During paper production, they act as retention aids and improve dry strength of paper products (Sharma et al., 2020). The most crucial step in the use of cationic starches in the wet-end is how they can be solubilized within a short time, while using lowest possible amount of resources. In food industry, autoclavation has been proposed for native starch dissolution, resulting in potential formation of resistant starches and products with adjustable properties e.g., stickiness and texture (Dundar & Gocmen, 2013; Li, Lei, et al., 2019; Li, Yu, et al., 2019). For CS however, the state-of-the-art technology in paper industry to solubilize cationic starches is to use steam-jet-cooking. In such steam jet-cookers, hot steam (typically with a temperature between 110 and 135 °C) breaks up starch granules. As this creates high shear forces in such devices, starches subsequently dissolve within a few minutes (Dintzis & Fanta, 1996) and can be operated in a continuous fashion. Afterwards, the solutions are diluted and applied to the pulp fiber slurries that contain other additives. Recently, we showed that jet-cooking conditions impact retention of cationic starches on pulp fibers (Ferstl et al., 2020). For dry cationized potato starches, for instance, a temperature of 115 °C yielded maximum retention on the pulp fibers (ca. 90%) while higher cooking conditions, e.g., 125 °C led to 80% retention. However, the other investigated potato starches featured the same trend but to a lesser extent. In a paper mill, the optimum conditions for the cooking process are difficult to establish and mainly rely on the experience of the operators and are often guided by trial and error. This originates from challenges to assess the solubility state of CS solutions in a process routine in combination with the lack of extensive scientific literature on this applied topic. As steam jet-cooking is an energy intense process, any savings in cooking conditions, have a large economic (less energy and/or starch needed) and subsequently also ecologic impact (less CO_2 produced). As CS is used in large amounts in the wet-end (0.7–8.0% per dry pulp), the cooking procedure is an interesting

☆ Members of the European Polysaccharide Network of Excellence (EPNOE).

* Corresponding author at: Institute of Bioproducts and Paper Technology, Graz University of Technology, Graz, Austria.
E-mail address: stefan.spirk@tugraz.at (S. Spirk).

https://doi.org/10.1016/j.carbpol.2022.119262
Received 3 December 2021; Received in revised form 25 January 2022; Accepted 14 February 2022
Available online 17 February 2022

target to improve the economic and ecologic performance of a paper mill.

Published papers on properties of jet-cooked starch solutions are scarce (Modig et al., 2006). Even for native starches, the scientific literature is not exhaustive despite the importance of steam jet-cooking to prepare aqueous starch solutions in different industrial context (de la Rosa-Millán et al., 2020; Ferng et al., 2011; Klem & Brogley, 1981). Depending on the conditions, degradation of the amylose/amylopectin backbones may occur, thereby decreasing the degree of polymerization (Byars, 2003). Some authors focused on cooling conditions of jet-cooked solutions and investigated the formation of spherulites and their inclusion complexes (Fanta et al., 2002). Such composites can be produced with a variety of materials (e.g., lipids) and have promising applications in different fields (Davies et al., 1980; Fanta et al., 2001; Fanta et al., 2002; Fanta et al., 2012; Fanta & Eskins, 1995). One of the most thorough papers on jet-cooking cationic starch solutions was published by Modig et al. (2006). They used asymmetric field flow fractionation to investigate the properties of amylopectin-rich cationic starch solutions (Modig et al., 2006). They demonstrated that jet-cooking reduced molar mass of CS significantly when increasing temperature above 130 °C. However, the authors did not focus on the solution state of the cationic starches.

Here, we aim at extending the knowledge of steam jet-cooking of industrial cationic starch samples in the context of rheology. In contrast to a previous report (Ferstl et al., 2020) where we focused on the retention of jet-cooked potato and corn starches on pulp fibers, here we assess the solubility state of these starches directly after steam jet-cooking and after storage. We explore the effect of temperature on the rheological behavior and support the results with optical microscopy studies. Rheology and in particular the knowledge on linear viscoelastic and thixotropic behavior can be employed as tools to design more efficient cooking procedures of CS in an industrial context.

2. Materials and methods

2.1. Materials

Sodium chloride was obtained from VWR Chemicals (>99%) and potassium chloride was obtained from Fluka Analytical (>99%). Cationic starches were obtained from different commercial suppliers. Information related to these starches is given in Table 1.

2.2. Preparation of starch solutions

2.2.1. Typical procedures for jet-cooking cationic starch samples

Cationic starch powder (adjusted to the dry weight of the respective starch) was transferred into a 25 L plastic container and water (5 L, ionic strength of 3 mM, prepared by dissolving NaCl and KCl in a 3:1 M ratio in deionized water) was added. The container was closed, shaken vigorously, and the starch slurry was transferred into the storage vessel (capacity 50 L) and stirred at 50 min^{-1} with a EUROSTAR 20 stirrer to prevent sedimentation. The storage vessel was connected to a Netzsch Mohno pump (type NM021BY02S12B) with adjustable flow rates up to 50 $L{\cdot}min^{-1}$. To adjust the pressure of the slurry inlet stream, a Jordan GP valve was used. A hydro THERMAL M101 hydroheater reaction chamber was used to mix the steam with the slurry inlet stream. The steam was generated by a PONY GE20/04P steam generator operating at pressures between 0.1 and 6.0 bar. The flow rate was set to 0.6 $L{\cdot}min^{-1}$at a pump frequency set to 9.7 Hz. The starch slurry was then cooked at temperatures between 120 and 130 °C. Residence time of the starch slurry in the heating element of the jet cooker was 90 s. Afterwards, the starch solutions were transferred to thermos bottles to keep heat loss as low as possible prior to further characterization using rheology. The solutions never reached a temperature below 85 °C. After sampling for rheology measurements, the solutions were placed in a drying oven in a closed preheated vessel overnight at 85 °C.

Table 1
Information on the investigated cationic starches employed in this study.

Origin	Cationization	Supplier	Dry weight	DS	ζ [mV]	Sample ID
Potato	Wet	Südstärke	85.1%	0.055	+30.1 ± 0.5	PW
Potato	Dry	Roquette	83.6%	0.045	+15.2 ± 0.2	PD
Corn	Wet	Agrana	88.4%	0.030	+22.5 ± 0.4	CW
Corn	Dry	Roquette	87.5%	0.030	+15.3 ± 0.1	CD

The solid content of the solutions after cooking was determined with a Mettler Toledo HR73 moisture analyser. The measurement was performed at a drying temperature of 140 °C. The amylose/amylopectin ratio after jet-cooking was determined using iodine colorimetry (Hovenkamp-Hermelink et al., 1988).

2.3. Rheology

The rheological characterization was performed on an Anton Paar MCR 502 (Anton Paar GmbH, Graz, Austria) rotational rheometer using a standard concentric cylinder measuring geometry (CC27) with a diameter of the inner rotating cylinder of 26.7 mm and cup diameter of 28.92 mm, combined with a standard Peltier temperature device (C-PTD200). Prior to each measurement, the samples were allowed to relax for 10 min. The frequency sweep, strain amplitude sweep, and flow curve were determined in this order in a single measurement series. Details for each test are given below.

2.3.1. Cooling curve

The measurement system was preheated to 90 °C before the sample was placed on the rheometer. Prior to measurements, the starch solutions were allowed to relax for 10 min at 90 °C followed by pre-shearing at a constant shear rate of $\dot{\gamma} = 10\ s^{-1}$ for a period of 3 min. The measurement was started at 90 °C and the final temperature (25 °C) was reached via a linear temperature ramp (-1 °C·min^{-1} at $\dot{\gamma} = 25\ s^{-1}$).

2.3.2. Frequency sweep, amplitude sweep and hysteresis loop tests

Before sample deposition, the temperature of the system was adjusted to 50 °C and kept constant for all the experiments. For the frequency sweep, the sample was pre-sheared at a shear rate $\dot{\gamma} = 25\ s^{-1}$ for 1 min followed by an oscillatory shear motion with a shear amplitude of γ_0= 18% and angular frequency of $\omega = 100$ rad·s^{-1} for 1 min. The angular frequency was decreased from 200 to 0.1 rad·s^{-1} (logarithmic ramp) at a constant shear strain amplitude of $\gamma_0 = 18\%$. For the strain amplitude sweep, the sample was pre-sheared at $\dot{\gamma} = 0.05\ s^{-1}$ for 2 min. The strain amplitude was increased from 0.01 to 100% (logarithmic ramp) at a constant ω = rad·10 s^{-1}. The linear viscoelastic region was determined based on preliminary tests and the strain sweep tests were herein included as a confirmation thereof. For the hysteresis loop tests, the sample was pre-sheared at $\dot{\gamma} = 0.05\ s^{-1}$ for 1 min. The shear rate was increased from 1 to 4950 s^{-1} (logarithmic ramp) within 150 s, held at 4950 s^{-1} for 50 s and was then decreased from 4950 to 1 s^{-1} (logarithmic ramp) within 150 s.

The complex viscosity functions obtained during the frequency sweep tests have been fitted using the well-known Carreau-Yasuda, Eq. (1), and Power law, Eq. (2) models (Barnes et al., 1989) depending on whether the functions showed the existence of a zero-shear viscosity plateau or not:

$$|\eta^*| = |\eta_0^*|(1 + \lambda\,\omega^a)^{\frac{n-1}{a}} \quad (1)$$

$$|\eta^*| = K\,\omega^{n-1} \quad (2)$$

with $|\eta^*|$ and $|\eta_0^*|$ being the complex viscosity and zero-shear complex viscosity magnitudes, respectively, and λ, a, n, K the fit parameters of the respective models.

2.4. Optical microscopy

Optical microscopy was performed on a polarization light microscope from Leica (Wetzlar, Germany) equipped with a thermo-controllable heating stage (precision 0.5 °C). In a typical experiment, the jet-cooked starch samples were deposited on preheated (95 °C) cover glass slides (Merck, 22 × 22 mm^2) and immediately covered with another preheated cover glass slide. Measurements were repeated by depositing solutions of the starches on the rheometer after storage for 12 h.

2.5. Zeta-potential

The zeta potential of starch solutions (c = 1 $mg{\cdot}ml^{-1}$, 25 °C) was determined using a Litesizer 500 using two electrode setup (Anton Paar GmbH, Graz, Austria). The Kalliope™ software was used for measurement and data evaluation. The cumulant model ISO 22,412 was used for the calculation of the mean hydrodynamic diameter. The analysis of the zeta potential was performed by applying the Smoluchowski approximation with a Debye factor of 1.50.

3. Results and discussion

3.1. Results

After cooking using different parameters, care was taken to avoid cooling of the sample below 85 °C as this can lead to irreversible changes in structure caused by retrogradation. The cooked slurries were transferred to thermally insulated bottles and stored until rheological characterization. The solutions were placed into the preheated system before the measurements were performed as described in the experimental section. The samples were characterized by rheology directly after cooking as well as after a storage time of 12 h.

3.1.1. Cooking temperature of 125 °C

The cooling curve (Fig. 1) for the starches cooked at 125 °C showed that the viscosity at 90 °C is similar for all samples (0.040–0.070 Pa·s).

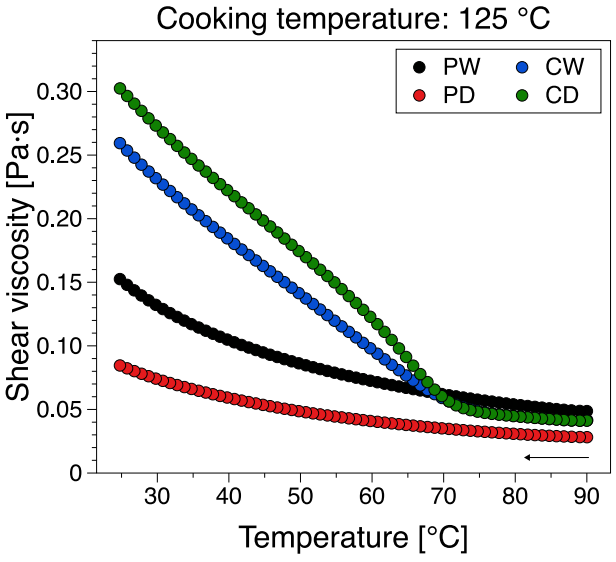

Fig. 1. Evolution of viscosity upon cooling (1 °C•min^{-1}, 25 s^{-1}) of jet-cooked cationic starch solutions (125 °C, 3.5 wt%, I = 3 mM).

Upon cooling below 75 °C, however, distinct differences evolved. The CW and CD samples exhibited a strong increase in viscosity indicating interactions between the macromolecules and retrogradation. The PW and PD samples, however, showed comparatively less increase in viscosity during cooling which indicated that these samples may already be dissolved at this cooking temperature, see the discussion of the results ahead.

The frequency sweep of the cationized potato and corn starch samples differed significantly (Fig. 2). PD and PW are characterized by a viscous dominated rheological material response, with $G'' > G'$ at all angular frequencies, Fig. 2.A. This can be taken as a further indication that the PD/PW samples had been solubilized at 125 °C cooking temperature. Their (complex) viscosity functions are qualitatively similar, comprising two regions, a plateau region and a shear-thinning region. They are comparable in magnitude, the viscosity being slightly higher for PD in the low angular frequency range, i.e. towards the zero-shear viscosity plateau, while practically identical in the shear thinning region, where conformational changes occur. In contrast, CW and CD show a more complex behavior. Both show a gel-like rheological response, with $G' > G''$ at lower angular frequencies indicating significant interactions/aggregation between the macromolecules, while at the higher angular frequencies $G' < G''$ suggesting that the gel-like interaction was disrupted by oscillation induced macromolecular conformational changes. The change in rheological response (where $G' = G''$) occurred at $\omega \approx$ 9 $rad{\cdot}s^{-1}$ for CW and $\omega \approx$ 29 $rad{\cdot}s^{-}$ for CD. In addition, while the viscosity function of CD indicated the existence of a zero-shear viscosity plateau, CW showed an increase in viscosity for ω<2 $rad{\cdot}s^{-1}$, suggesting the existence of a yield-stress. The testing of the solutions 12 h after cooking is shown in Fig. 2.B,D. The PD and PW samples did not show any significant qualitative and quantitative changes in material response. In contrast, CW and CD showed significant changes in behavior 12 h after cooking. CW exhibited a liquid-like behavior, $G'' > G'$, over the entire angular frequency range accompanied by a decrease in viscosity of almost 1 decade, and also exhibiting an apparent zero-shear viscosity plateau. CD showed a qualitatively similar behavior in dynamic moduli, however, with an increase in the liquid-gel transition ($G' = G''$) to $\omega \approx$35 $rad{\cdot}s^{-1}$.

The strain amplitude sweep data (Fig. S1, SI) essentially confirm the frequency sweep data (compare datapoints with ω=10 rad s^{-1} and γ_0= 18% between the two datasets). Furthermore, all data confirms that the frequency sweep measurements were performed in the linear viscoelastic regime.

The hysteresis loop tests are presented in Fig. 3. For all samples, the shear stress increase with shear rate confirms their shear thinning behavior, see also (Fig. S2, SI). Similar to the previous tests, negligible differences were recorded between PW and PD before and after cooking. Interestingly, the shear stresses on the downward curve (decreasing shear rate) are higher than on the upward curve (increasing shear rate). This highlights an apparent anti-thixotropic (rheopectic) behavior. While for thixotropic samples in hysteresis loop tests samples experience gradual de-structuring on the upward curve rendering the shear stress/viscosities lower on the downward curve, and anti-thixotropic behavior implies a 'thickening' behavior, generally attributed to the tendency of polymer molecules to aggregate in solution giving rise to temporary aggregates (Buitenhuis & Pönitsch, 2003). From molecular point of view this has been attributed to θ solvents, tacticity effects influencing solubility and linking of polymer molecules by small amounts of unknown contaminants, among others (Buitenhuis & Pönitsch, 2003). We have to also caution against other possible artefacts such as the presence of a complex shear history of the samples, and the highly transient conditions in which the thixotropic loop tests were performed. Interestingly, not all samples studied displayed anti-thixotropic behavior. Directly after cooking, CW showed almost no anti-thixotropic behavior while CD shows an anti-thixotropic behavior below 70 s^{-1}. In contrast, 12 h after cooking CD showed no apparent time-dependent behavior while exhibited anti-thixotropic behavior similar to PW and PD. These

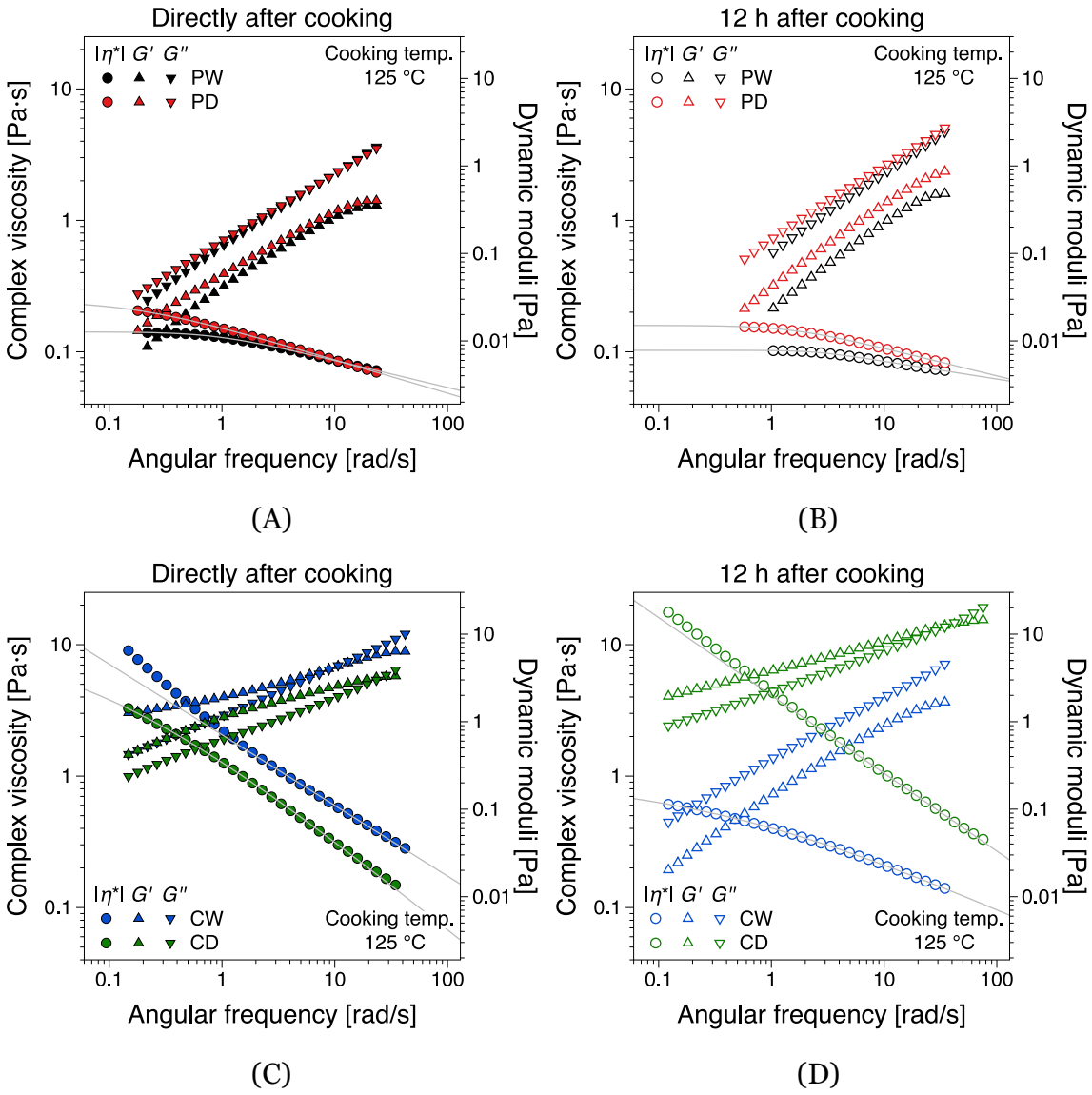

Fig. 2. Frequency sweep tests ($\gamma_0 = 18\%$, 50 °C) of jet-cooked cationic starch solutions (125 °C, 3.5 wt%, $I = 3$ mM) directly after cooking (A, C) and after 12 h of storage at room temperature (B, D). The continuous lines are complex viscosity (magnitude) function fits according to Eqs. (1)–(2).

rheological results were confirmed by optical microscopy observations of the starch solutions directly after cooking and after storage for 12 h. The PW and PD samples appear fully dissolved with hardly any particles visible in the microscopy images. The CW and CD samples showed a variety of particles in the samples, that could classify as remnants. Interestingly, the remnants remain for the CD sample while they disappear for the CW samples during storage, which is in agreement with rheology solubility assessment. It appears in the microscopy images for CW that the previously present remnant particles gelatinize and hardly any particles can be identified in the images after storage for 12 h (Fig. 4).

3.1.2. *Influence of cooking temperature*

According to the dynamic moduli in the 120 °C data PD and PW are already dissolved at 125 °C, therefore, higher temperatures have not been considered as that would lead to degradation of the cationic starches. However, for CD and CW, higher temperatures would be needed for complete dissolution, see also Fig. 2C,D. Therefore, other cooking temperatures (PD/PW: 120 °C; CD/CW: 130 °C) were selected.

Fig. 5 depicts the cooling curves of the four starches cooked at 120 (PD/PW) and 130 °C (CD/CW). The initial viscosity (at 90 °C) was hardly affected by the cooking temperature and is in the same order of magnitude as for the samples cooked at 125 °C. Significant differences occurred below 60 °C with CD/CW samples having lower viscosities and PD/PW comparable (CD) or higher than the samples cooked at 125 °C, see Fig. 1.

While PD showed just a slight increase in viscosity at 25 °C (from 0.07 to 0.9 Pa•s), PW increased to a larger extent (from 0.15 to 0.21 Pa•s). The difference in PW and PD viscosities between the cooking temperatures can be due to a higher starting viscosity (90 °C) for PW cooked at 120 °C as the relative change in viscosity over the temperature range is very similar. Both corn starches behaved similarly with a reduction of viscosity at 25 °C from 0.30 to 0.16 Pa•s (CD) and 0.27 to 0.19 Pa•s (CW). However, the cooling viscosity curves, indicating rearrangements during cooling (retrogradation, starting from 65 °C), remained very similar to those at 125 °C cooking temperature.

The frequency sweep experiments (Fig. 6) showed that the PD and PW samples still featured $G'' > G'$ over the whole frequency range. Storage did not significantly impact the material response. Interestingly, the frequency sweep experiments showed that CW and CD featured $G' >$

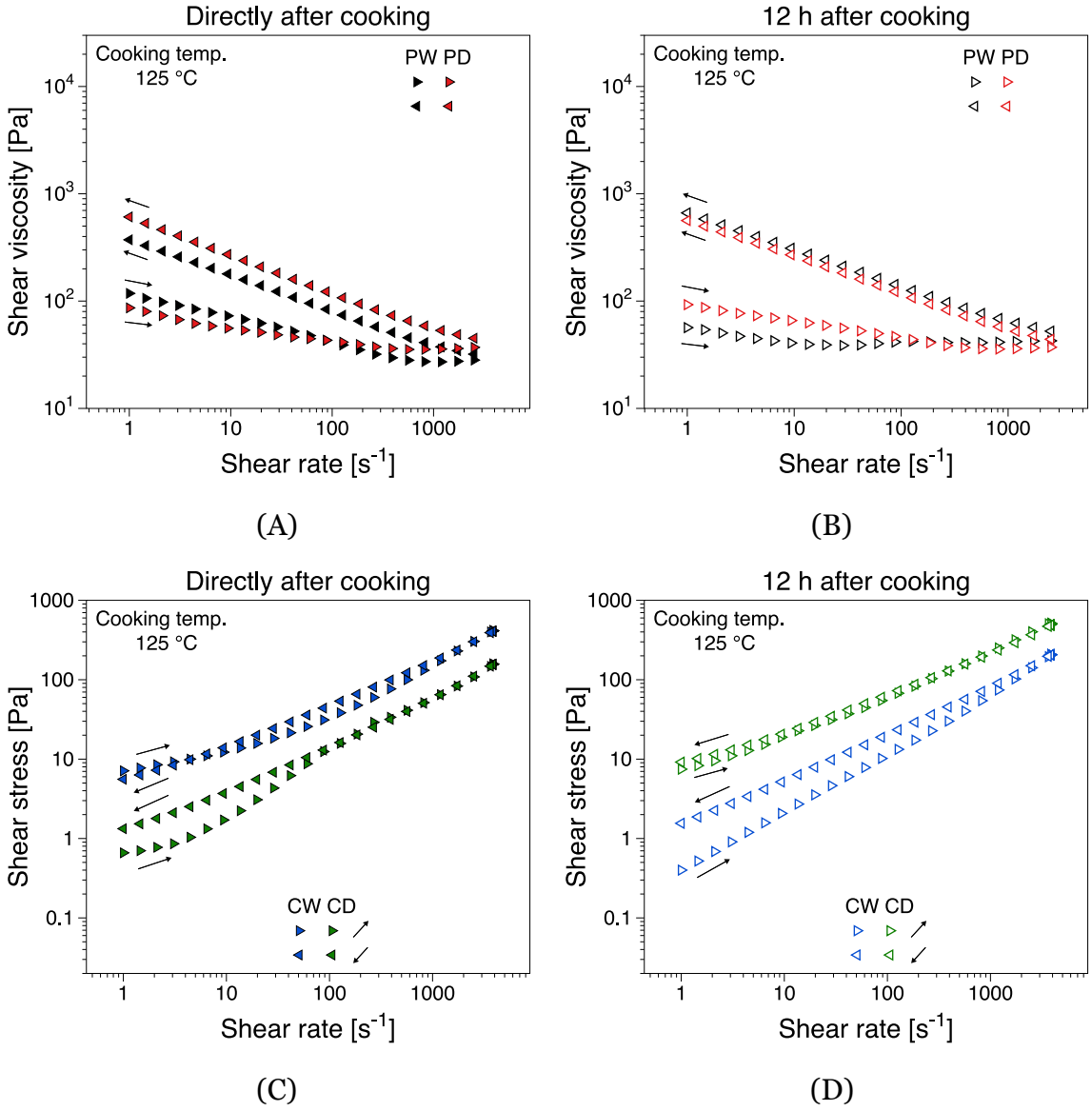

Fig. 3. Hysteresis loop flow curves (50 °C) of jet-cooked cationic starch solutions (125 °C, 3.5 wt%, $I = 3$ mM) directly after cooking (A, C) and after 12 h of storage at room temperature (B, D).

G'' at low to medium angular frequencies. The transition from gel-like behavior occurred at approx. 20 rad s^{-1} for both samples directly after cooking. The 12 hours storage time revealed the same characteristics as for the cooking experiments performed at 125 °C. The CW sample featured $G'' > G'$ over the whole angular frequency range. The CD sample showed $G' > G''$ at low angular frequencies (<1 rad s^{-1}) albeit the difference was rather small. From 1 to 6 rad s^{-1} the dynamic moduli were approximately equal, whereas above 6 rad s^{-1} $G'' > G'$.

The corresponding amplitude sweeps (Fig. S3, SI) showed similar profiles as the samples cooked at 125 °C and essentially confirm the frequency sweep data both qualitatively and quantitatively. Also similarly, Furthermore, all data confirms that the frequency sweep measurements were performed in the linear viscoelastic regime.

The hysteresis loop tests showing the influence of cooking temperature are presented in Fig. 7. Similarly to the data in Fig. 3, the shear stress variation with increasing shear rate confirms their shear thinning behavior, see also (Fig. S4, SI). The differences between PW and PD directly after cooking and 12 h after cooking continued to be negligible. As for the PW and PD samples cooked at 125 °C, Fig. 3, the hysteresis loop tests show an apparent anti-thixotropic behavior. Interestingly, increasing the cooking temperature to 130 °C caused CW to become thixotropic while CD showed almost no hysteresis directly after cooking. In contrast, 12 h after cooking the CW and CD behavior at 130 °C is very similar to 125 °C with CW showing anti-thixotropic behavior and CD showing almost identical shear stresses on the upward and downward curves.

3.2. Discussion

Steam jet-cooking is a very peculiar form of solubilization of starch. In contrast to heating starches on a hot plate or in batch cookers, steam is not only heating the slurry to temperatures above 100 °C but is also penetrating the granules at high speed (pressure: 2–3 bar in our experiments) causing mechanical stress (Ferng et al., 2011). Disintegration of the granules is therefore more effective (Fig. 8) and proceeds within a few minutes.

In our case, the residence time of the cationic starches in the cooker was 90 s before the solutions were collected. As heating proceeds fast, disintegration may also immediately affect the crystalline domains (cleavage of hydrogen bonds, helix unwinding), while diffusion

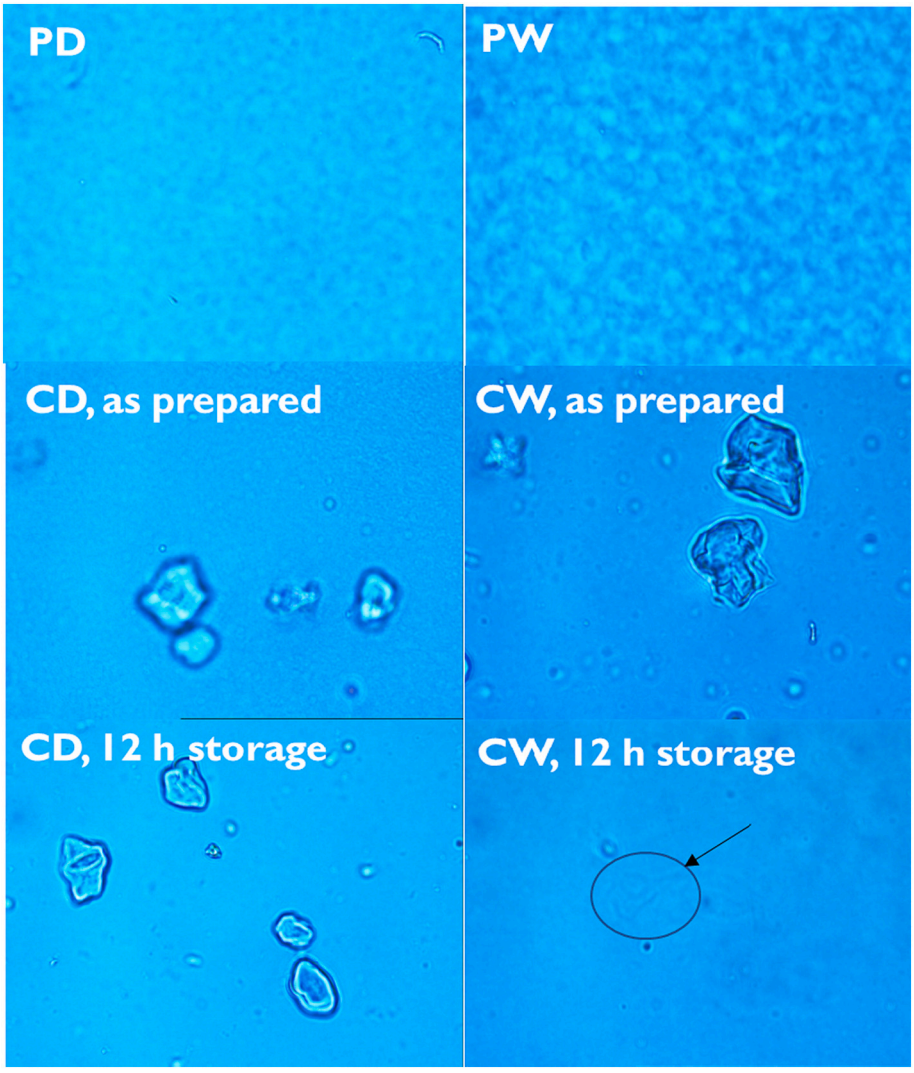

Fig. 4. Optical microscopy images (50×) of the different starch samples jet-cooked at 125 °C (I = 3 mM, c = 3.5 wt%). The freshly prepared solutions were applied to hot cover slides. Images were acquired at 95 °C.

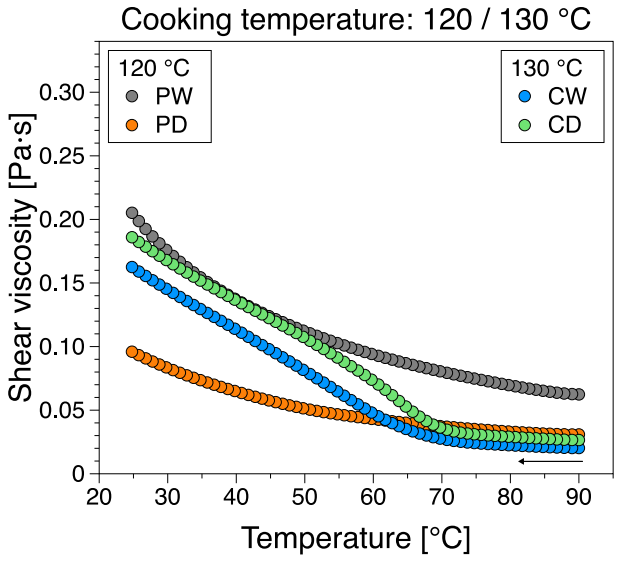

Fig. 5. Evolution of viscosity upon cooling of jet-cooked cationic starch solutions (3.5 wt%, *I* = 3 mM) at 120 °C (PW/PD) and 130 °C (CW/CD).

processes (e.g. of water into amorphous domains), important in conventional gelatinization to swell the granules, play a minor role (Jenna et al., 2018; Ritota et al., 2008). In the case of jet-cooking, enthalpic contributions may dominate as the system cannot relax under pressure and high shear. The arrangement of the helices and their accessibility to water inside the crystal structure therefore largely affects the dissolution of the starches (Fig. 9). *A-type,* monoclinic starches for instance feature densely packed helices with hardly any space between the helices for water. *B-type* hexagonally packed starches on the other hand have a large cavity, where much more water can be intercalated than in *A-type* starches (Le Corre et al., 2010). We speculate here whether this is one of the reasons why the CD and CW (*A-type*) feature a worse solubility behavior than the PW/PD (*B-type*) samples.

Model studies with defined non-charged starches showed that the transition from ordered-to-disordered regime required much higher temperatures for *A-type* than for *B-type* starches (Crochet et al., 2005). Using rheology, we were able to track the differences between the cationic starches during steam jet-cooking. A summary of several representative rheological parameters is presented in Fig. 10. We observed that the shear viscosity at room temperature generally decreased by increasing the cooking temperature, compare Figs. 1 and 5. This indicated less interactions between molecules either by solvation or, to some extent, by cleavage of glycosidic bonds as described in

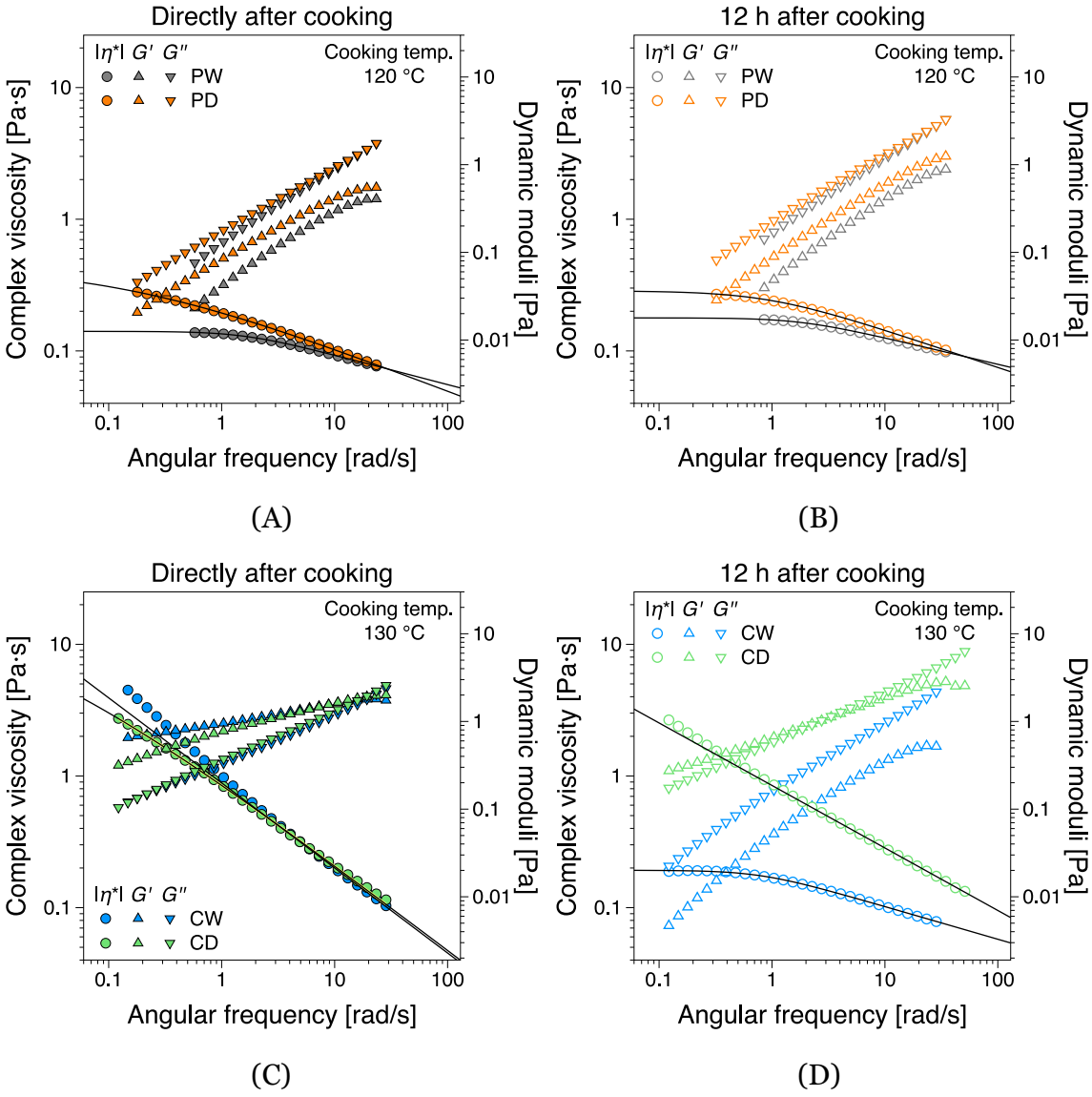

Fig. 6. Frequency sweep experiment ($\gamma_0 = 18\%$, 50 °C) of jet-cooked cationic starch solutions (PD, PW: 120 °C, CD, CW: 130 °C, 3.5 wt%, $I = 3$ mM) directly after cooking (A, C) and after 12 h of storage at room temperature (B, D). The continuous lines are complex viscosity (magnitude) function fits according to Eqs. (1)–(2).

another report (Modig et al., 2006). The corn cationic starches CW and CD featured some form of retrogradation during the cooling of the sample in the rheometer, indicated by a sharp increase in viscosity at 60–65 °C. Retrogradation is a diffusion-controlled process as amylose and amylopectin molecules tend to reassemble into single and double helices, respectively, followed by further aggregation phenomena (e.g., crosslinking of crystallites) (Lu et al., 2011). Typically, the time scale of this process is hours (amylose) to even days (amylopectin) (Kovrlija & Rondeau-Mouro, 2017). This is much longer than the time we allowed the system to relax as we used a cooling ramp of 1 °C min^{-1}, i.e. the solutions reached a temperature of 60 °C after ca. 30 min, which is rather short to develop significant retrogradation. However, we observed aggregation during cooling for both corn starches. There are several factors which can enhance retrogradation (minor acidity, increasing fat content, impurities and polyvalent ions, amylose rich starches) (Smits et al., 2003). Probably, the presence of remnants, often also called ghost particles (Derek et al., 1992; Zhang et al., 2017), is responsible for the retrogradation of the CW and CD samples. While the CD samples remained relatively unchanged upon storage, the rheological properties of the wet-cationized corn starch, CW, sample showed remarkable alterations, compare Figs. 2 and 6, (B,D), both quantitatively and qualitatively. Thus, the complex viscosity decreased by almost two orders of magnitude at low angular frequencies 12 h after cooking for both 125 °C and 130 °C, see e.g., K in Fig. 9. Furthermore, while directly after cooking the dynamic moduli indicate a gel-like behavior ($G' > G''$) up to approximately 9 rad s^{-1} for the sample cooked at 125 °C and 20 rad s^{-1} for the sample cooked at 130 °C, 12 h after cooking the CW shows a liquid-like behavior ($G'' > G'$) for the entire frequency range, see the crossover frequency $\omega|_{G'=G''}$ in Fig. 10. We could not find a similar case for jet-cooked samples in literature. A potential explanation involves the dissolution of some remnants, which remained in the solutions after jet-cooking. As mentioned above, jet-cooking uses strong forces to disintegrate the granules. If a few of such granules remained partially intact, they may start to swell during storage for 12 h, and finally lead to gelatinized samples by applying shear during the rheological experiments. This would then result in the observed phenomenon of $G'' > G'$ in both frequency and amplitude sweep experiments. It is interesting that even at a cooking temperature of 135 °C, the CW sample (data not shown) showed the same rheological behavior (after cooking: $G' > G''$; after storage for 12 h: $G'' > G'$).

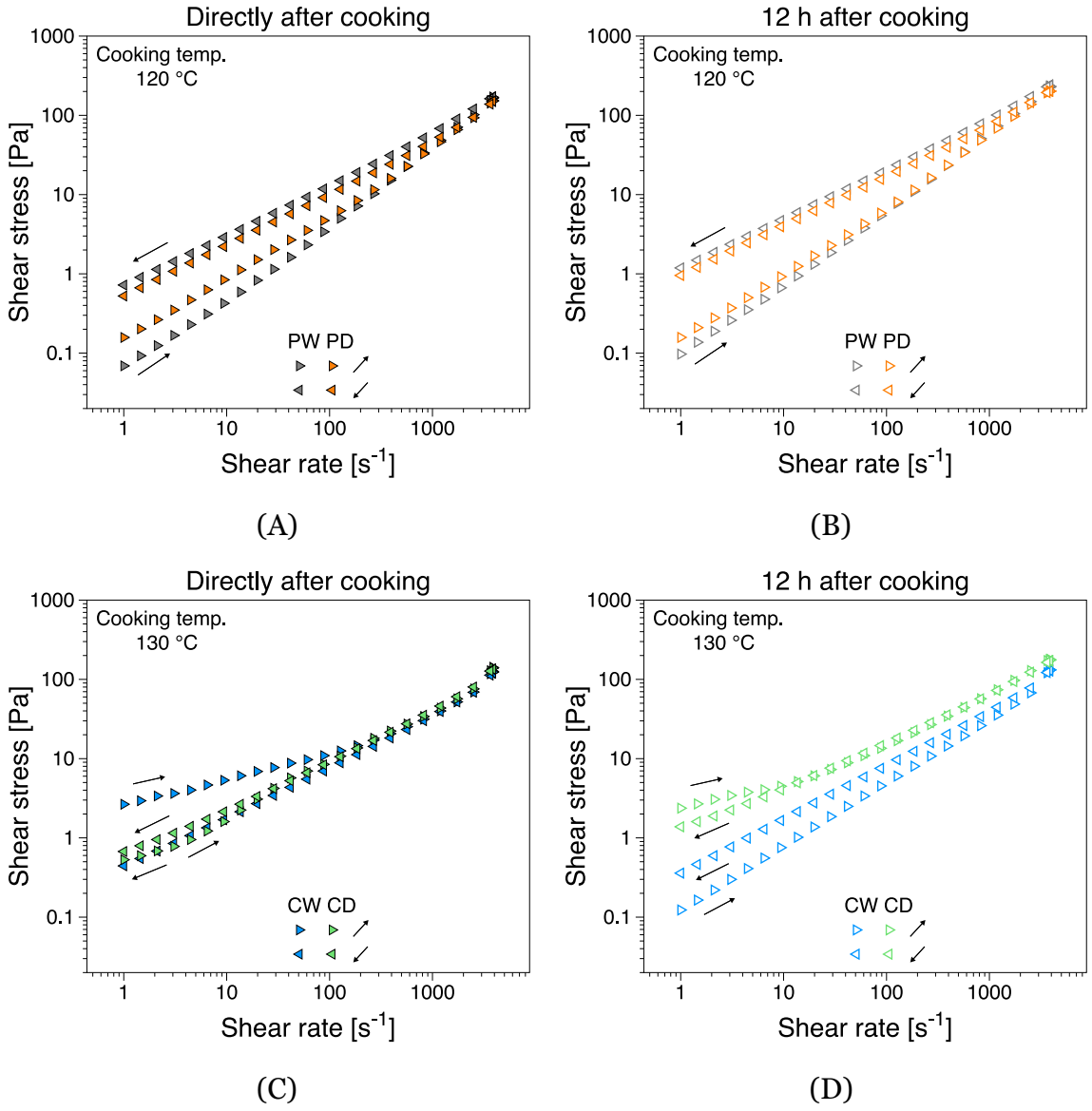

Fig. 7. Hysteresis loop flow curves (50 °C) of jet-cooked cationic starch solutions (PD, PW: 120 °C, CD, CW: 130 °C, 3.5 wt%, $I = 3$ mM) directly after cooking (A, C) and after 12 h of storage at room temperature (B, D).

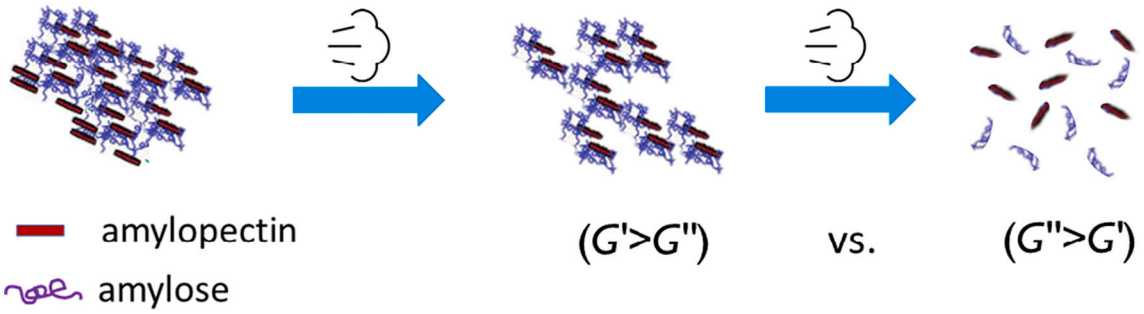

Fig. 8. Schematic representation of disintegration and solubilization of cationic starch during jet-cooking.

The thixotropic behavior also produced intriguing results. Independent of the cooking temperature, PW and PD showed anti-thixotropic flow curves. Such behavior has previously been associated to flow-induced gel-network formation or to the dynamics of an existing network (Buitenhuis & Pönitsch, 2003; Buitenhuis & Springer, 2003; Eliassaf et al., 1955; Ohoya et al., 2000; Quadrat, 1985; Quadrat et al., 1992). For both hypotheses, the molecular origins of the behavior has yet to be elucidated (Buitenhuis & Pönitsch, 2003; Buitenhuis & Springer, 2003). In the context of the present study, the anti-thixotropic behavior has to be related to the solubility of the starches. Considering

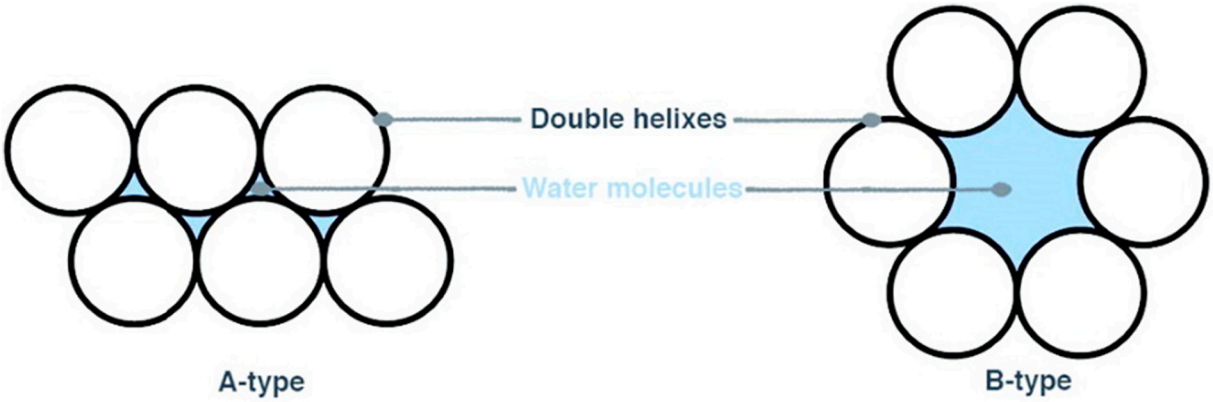

Fig. 9. Arrangement of helixes in the crystalline starch domains.
Reproduced from (Le Corre et al., 2010) with permission of the American Chemical Society.

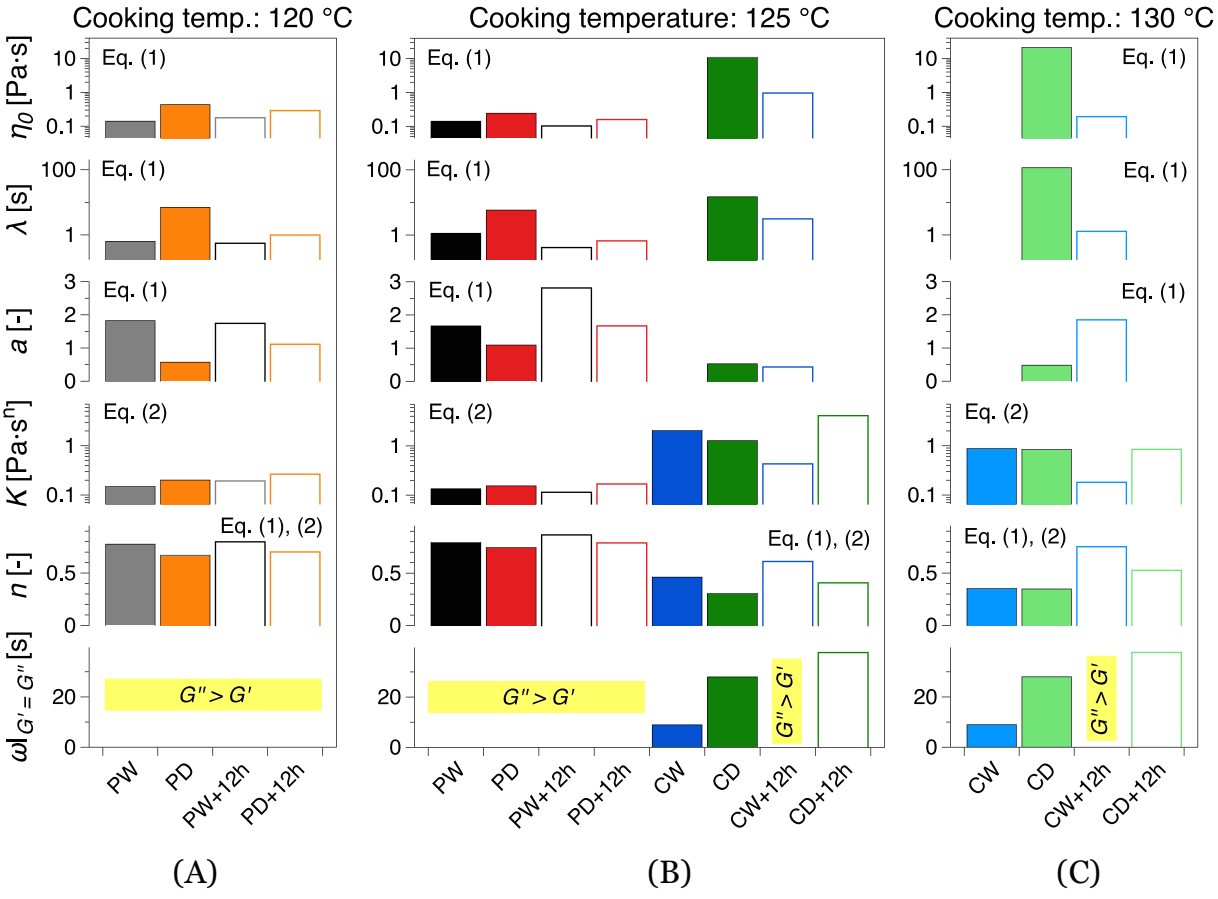

Fig. 10. Summary of characteristic rheological parameters, i.e. fitting parameters from Eqs. (1)–(2) and the crossover frequency, $\omega|_{G'=G''}$, comparing data from cationic starches cooked at (A) 120 °C – PW, PD (B) 125 °C and (C) 130 °C – CW, CD. Filled bars corresponds to the tests directly after cooking while hollow bars correspond to tests 12 h after cooking.

the well-solubilized (B-type in Fig. 9) PW and PD, they both disclose a clear and storage-independent anti-thixotropic behavior, irrespective of the investigated cooking temperature. Considering that in dynamic frequency sweep tests both exhibit liquid-like behavior ($G'' > G'$) presumes the absence of a starting gelled network in the hysteresis loop tests and therefore it could be inferred that a shear-induced gelled network could be formed. In contrast, CW had negligible time-dependence while CD is significantly influenced by the storage time and cooking temperature. When cooked at 125 °C, CW showed hardly any time-dependence directly after cooking while 12 h thereafter it showed anti-thixotropic behavior. Increasing the cooking temperature to 130 °C, showed a clear thixotropic behavior directly after cooking whereas 12 h after cooking there was again a clear anti-thixotropic behavior, similar to PW and PD. This further supports the premise that some of the granules may remain partially intact in CD and CW after cooking.

The amylose/amylopectin ratio (Fig. S5, SI) determined by iodine colorimetry showed two remarkable properties of the starches. Prior to

jet-cooking, the amylose contents for the dry cationized samples are higher than for the corresponding wet cationized ones (PD 34.6% vs. PW 27.5%; CD: 30.6% vs. 22.5%). The ratio changed after jet-cooking (125 °C, 3.5 wt%) to lower but similar levels ranging from 16.9 ± 0.8% (CW) to 21.2 ± 0.1% (PD). In literature, alterations of amylose/amylopectin ratios determined by iodine colorimetry have been assigned to a variety of factors (Vilaplana et al., 2012), with the dissolution technique being explicitly mentioned (Mahmood et al., 2007). In the course of steam jet-cooking, the liberation of internal lipids from the starches may interfere with the formation of the amylose-iodine complexes, leading to lower effective amylose contents (Morrison & Laignelet, 1983).

Retrogradation of the other samples during storage is retarded as the cationic charges (zeta potentials between +15 to +30 mV) lead to repulsion of the macromolecules. As at the present ionic strength (3 mM) there is already some screening of the charges between cationic segments on the macromolecule backbone, CD, PD and PW solutions did not show any signs of aggregation upon storage for 12 h and CW even proceeded to liquid like state during storage.

4. Conclusion

The solubilization of starch is a complex process as many parameters are non-linearly linked, making the interpretation of results as well as the design of experiments difficult. Here, we focused on the effect of jet-cooking on the rheological properties of industrial cationic starch samples by screening four different samples at several temperatures and constant ionic strength at a concentration of 3.5 wt%. We chose rheology because it is an excellent tool to study properties of polymeric systems in the solution state that yields data on macromolecular assembly which is hardly accessible by other techniques. We showed that at 120 and 125 °C cooking temperature all the potato starches have been solubilized while the corn starches still have a few insoluble parts (CW) or are not fully dissolved (CD) at the studied cooking temperatures. Probably, this is due to the different crystalline arrangement of helices leading to differences in accessibility between the corn and potato starches, respectively. Temperature has an effect but even at 135 °C the CW sample for instance still featured remnants while in addition, degradation may come into play as well. Further studies are required to fully assess more parameters that influence the outcome of the jet-cooking, such as change in starch concentration or variation of ionic strength, which would have gone beyond the scope of this paper.

CRediT authorship contribution statement

M. Gabriel: methodology, data curation, investigation, validation, **F. Gomernik**: Conceptualization, methodology, **E. Ferstl**: investigation, **A. Chemelli**: conceptualization, supervision, **R. Kádár**: data curation, visualization, writing- Reviewing and Editing, **S. Spirk**: writing - original draft preparation, writing- reviewing and editing, supervision, funding acquisition.

Declaration of competing interest

The authors declare that they have no known competing financial interests or personal relationships that could have appeared to influence the work reported in this paper.

Acknowledgements

The Austrian Research Promotion Agency (FFG) is gratefully acknowledged for financial support of the Stärke+ project (878306).

Appendix A. Supplementary data

Supplementary data to this article can be found online at https://doi.org/10.1016/j.carbpol.2022.119262.

References

Barnes, H. A., Hutton, J. F., & Walters, K. (1989). *An introduction to rheology*. Amsterdam, NL.: Elsevier.
Buitenhuis, J., & Pönitsch, M. (2003). Negative thixotropy of polymer solutions. 1. A model explaining time-dependent viscosity. *Colloid & Polymer Science, 281*, 253–259.
Buitenhuis, J., & Springer, J. (2003). Negative thixotropy of polymer solutions. 2. A systematic study of the time-dependent viscosity of partially hydrolyzed polyacrylamide. *Colloid & Polymer Science, 281*, 260–266.
Byars, J. A. (2003). Jet cooking of waxy maize starch: Solution rheology and molecular weight degradation of amylopectin. *Cereal Chemistry, 80*, 87–90.
Crochet, P., Beauxis-Lagrave, T., Noel, T. R., Parker, R., & Ring, S. G. (2005). Starch crystal solubility and starch granule gelatinisation. *Carbohydrate Research, 340*, 107–113.
Davies, T., Miller, D. C., & Procter, A. A. (1980). Inclusion complexes of free fatty acids with amylose. *Starch - Stärke, 32*, 149–158.
de la Rosa-Millán, J., Orona-Padilla, J. L., Flores-Moreno, V. M., & Serna-Saldívar, S. O. (2020). Effect of jet-cooking and hydrolyses with amylases on the physicochemical and in vitro digestion performance of whole chickpea flours. *International Journal of Food Science & Technology, 55*, 690–701.
Derek, R., Prentice, M., Stark, J. R., & Gidley, M. J. (1992). Granule residues and "ghosts" remaining after heating A-type barley-starch granules in water. *Carbohydrate Research, 227*, 121–130.
Dintzis, F. R., & Fanta, G. F. (1996). Effects of jet-cooking conditions upon intrinsic viscosity and flow properties of starches. *Journal of Applied Polymer Science, 62*, 749–753.
Dundar, A. N., & Gocmen, D. (2013). Effects of autoclaving temperature and storing time on resistant starch formation and its functional and physicochemical properties. *Carbohydrate Polymers, 97*, 764–771.
Eliassaf, J., Silberberg, A., & Katchalsky, A. (1955). Negative thixotropy of aqueous solutions of polymethacrylic acid. *Nature, 176*, 1119-1119.
Fanta, G. F., & Eskins, K. (1995). Stable starch—lipid compositions prepared by steam jet cooking. *Carbohydrate Polymers, 28*, 171–175.
Fanta, G. F., Felker, F. C., & Shogren, R. L. (2002). Formation of crystalline aggregates in slowly-cooled starch solutions prepared by steam jet cooking. *Carbohydrate Polymers, 48*, 161–170.
Fanta, G. F., Felker, F. C., & Shogren, R. L. (2012). Recent processing methods for preparing starch-based bioproducts. *Food and Industrial Bioproducts and Bioprocessing*, 37–83.
Fanta, G. F., Felker, F. C., Shogren, R. L., & Knutson, C. A. (2001). Starch–paraffin wax compositions prepared by steam jet cooking. Examination of starch adsorbed at the paraffin–water interface. *Carbohydrate Polymers, 46*, 29–38.
Ferng, L.-H., Chen, S.-H., & Lin, Y.-A. (2011). Effect of steam jet cooking on the destruction of corn starches. *Procedia Food Science, 1*, 1295–1300.
Ferstl, E., Gabriel, M., Gomernik, F., Müller, S. M., Selinger, J., Thaler, F., Bauer, W., Uhlig, F., Spirk, S., & Chemelli, A. (2020). Investigation of the adsorption behavior of jet-cooked cationic starches on pulp fibers. *Polymers, 12*, 2249.
Hovenkamp-Hermelink, J. H. M., De Vries, J. N., Adamse, P., Jacobsen, E., Witholt, B., & Feenstra, W. J. (1988). Rapid estimation of the amylose/amylopectin ratio in small amounts of tuber and leaf tissue of the potato. *Potato Research, 31*, 241–246.
Jenna, R., Ekaterina, N., & Yrjö, H. (2018). On-line monitoring of cationic starch gelatinization and retrogradation by 1H NMR-relaxometry. *Nordic Pulp & Paper Research Journal, 33*, 625–631.
Klem, R. E., & Brogley, D. A. (1981). Methods for selecting the optimum starch binder preparation system. *Pulp & Paper, 55*, 98–103.
Kovrlija, R., & Rondeau-Mouro, C. (2017). Hydrothermal changes in wheat starch monitored by two-dimensional NMR. *Food Chemistry, 214*, 412–422.
Le Corre, D., Bras, J., & Dufresne, A. (2010). Starch nanoparticles: A review. *Biomacromolecules, 11*, 1139–1153.
Li, H., Lei, N., Yan, S., Gao, M., Yang, J., Wang, J., & Sun, B. (2019). Molecular causes for the effect of cooking methods on rice stickiness: A mechanism explanation from the view of starch leaching. *International Journal of Biological Macromolecules, 128*, 49–53.
Li, H., Yu, L., Yu, W., Li, H., & Gilbert, R. (2019). Autoclaved rice: The textural property and its relation to starch leaching and the molecular structure of leached starch. *Food Chemistry, 283*, 199–205.
Lu, S., Chen, J.-J., Chen, Y.-K., Lii, C.-Y., Lai, P., & Chen, H.-H. (2011). Water mobility, rheological and textural properties of rice starch gel. *Journal of Cereal Science, 53*, 31–36.
Mahmood, T., Turner, M. A., & Stoddard, F. L. (2007). Comparison of methods for colorimetric amylose determination in cereal grains. *Starch - Stärke, 59*, 357–365.
Modig, G., Nilsson, P.-O., & Wahlund, K.-G. (2006). Influence of jet-cooking temperature and ionic strength on size and structure of cationic potato amylopectin starch as measured by asymmetrical flow field-flow fractionation multi-angle light scattering. *Starch - Stärke, 58*, 55–65.
Morrison, W. R., & Laignelet, B. (1983). An improved colorimetric procedure for determining apparent and total amylose in cereal and other starches. *Journal of Cereal Science, 1*, 9–20.
Ohoya, S., Hashiya, S., Tsubakiyama, K., & Matsuo, T. (2000). Shear-induced viscosity change of aqueous polymethacrylic acid solution. *Polymer Journal, 32*, 133–139.
Quadrat, O. (1985). Negative thixotropy in polymer solutions. *Advances in Colloid and Interface Science, 24*, 45–75.

Quadrat, O., Bradna, P., Dupuis, D., & Wolff, C. (1992). Negtive thixotropy of solutions of partially hydrolyzed polyacrylamide. Part I: The influence of shear rate on time changes of flow characteristics. *Colloid & Polymer Science, 270*, 1057–1059.

Ritota, M., Gianferri, R., Bucci, R., & Brosio, E. (2008). Proton NMR relaxation study of swelling and gelatinisation process in rice starch–water samples. *Food Chemistry, 110*, 14–22.

Sharma, M., Aguado, R., Murtinho, D., Valente, A. J. M., Mendes De Sousa, A. P., & Ferreira, P. J. T. (2020). A review on cationic starch and nanocellulose as paper coating components. *International Journal of Biological Macromolecules, 162*, 578–598.

Smits, A. L. M., Kruiskamp, P. H., van Soest, J. J. G., & Vliegenthart, J. F. G. (2003). The influence of various small plasticisers and malto-oligosaccharides on the retrogradation of (partly) gelatinised starch. *Carbohydrate Polymers, 51*, 417–424.

Vilaplana, F., Hasjim, J., & Gilbert, R. G. (2012). Amylose content in starches: Toward optimal definition and validating experimental methods. *Carbohydrate Polymers, 88*, 103–111.

Zhang, B., Selway, N., Shelat, K. J., Dhital, S., Stokes, J. R., & Gidley, M. J. (2017). Tribology of swollen starch granule suspensions from maize and potato. *Carbohydrate Polymers, 155*, 128–135.